DRF-06728

Haughey

REPORT NO. 584-4-214
CONTRACT NAS 8-21291

EVALUATION AND APPLICATION OF DATA FROM LOW-GRAVITY ORBITAL EXPERIMENT

SECOND QUARTERLY PROGRESS REPORT

GENERAL DYNAMICS
Convair Division

REPORT NO. 584-4-214

EVALUATION AND APPLICATION OF DATA FROM LOW-GRAVITY ORBITAL EXPERIMENT

SECOND QUARTERLY PROGRESS REPORT

27 September 1968

Prepared Under
Contract NAS8-21291

Prepared by
CONVAIR DIVISION OF GENERAL DYNAMICS
San Diego, California

FOREWORD

This quarterly progress report covers work performed under NASA/MSFC Contract Number NAS8-21291 during the reporting period 20 May - 20 August, 1968. Contract control number is DCN1-8-52-10101. Personnel contributing to this report include R. D. Bradshaw, project manager, M. H. Blatt, L. R. Kaszas, A. R. Marchese, and A. B. Walburn. This study is performed under the technical direction of Mr. Leon J. Hastings, NASA/MSFC, R-P&VE-PT.

TABLE OF CONTENTS

LIST OF FIGURES

NOMENCLATURE

A_c	cross sectional area of tank, sq ft
C	liquid specific heat, $\frac{BTU}{lb_m - {}^oR}$
H	height of tank, ft
h	liquid level height, ft
J	conversion constant, 778 $\frac{ft\text{-}lb_f}{BTU}$
m	liquid mass, lb_m
p	pressure, lb/sq in
Q_w	wall heat transfer, BTU
R_v	gas constant of vapor, $\frac{ft\text{-}lb_f}{lb_m - {}^oR}$
r	cavity radius, in
T	temperature, ^oR
β	fractional amount of entrained vapor
Δ	initial value minus final value
λ	heat of evaporation, BTU/lb_m
ρ	density, lb_m/cu ft
σ	liquid surface tension, lb_f/in
Ψ	ratio of superheated liquid mass to total liquid mass

SUBSCRIPTS

f	final
i	incipient boiling value
ℓ	liquid
o	initial
s	saturated
v	vapor

MISCELLANEOUS

$'$	superheated
$\overline{(\ )}$	average of ( )

SUMMARY

This report contains work performed at Convair during the second quarterly period of the study "Evaluation and Application of Data From Low Gravity Orbital Experiment." This report contains a discussion of analytical work in the areas of repressurization, thermal energy evaluation, tank pressure rise, liquid level rise, and dynamics of sloshing.

Valid modeling of the repressurization period of flight involves specifying of several variables. These include a time-dependent helium input thermodynamic state, the thermodynamic interactions of the recirculation flow, and the tank wall thermal energy input. These variables are being investigated; some difficulty has occurred in the thermal modeling of the S-IVB forward bulkhead area.

The evaluation of the pressure rise during the fourth orbit closed tank experiment has also been complicated by difficulty in defining the thermal energy input through the forward bulkhead. Present comparisons indicate current thermal modeling is grossly under predicting this area of energy input. Forward dome absorptivities are being analyzed as are the effects of thermal conductivity variation. Results with the thermodynamic program predicting pressure rise rate have bracketed the flight results, however the ullage energy input simulation is still subject to question.

A mathematical formulation has been developed to evaluate the change in liquid level height during a rapid vent down. A discussion is given

of the previous models for this event and their shortcomings. The contributions from saturated boiling caused by a change in saturation pressure, wall heat transfer during the blowdown, and the occurrence of liquid superheat are analyzed for the magnitude of their effect on liquid level rise. The latter two contributions are shown to normally be negligible for the AS-203 case. The significance of bubble retention times is discussed and parametric data is presented.

The application of the pendulum analogy for slosh simulation of model drop tower tests is discussed. The parameters have been defined for the 6-inch scale model AS-203 tank. Data on slosh amplitude, velocity, and acceleration will be used to determine correlations for amplification factor, effective propellant damping, and slosh period with Bond number and Froude number. These correlations from the analytical model with the scale tests will provide insight into full scale simulation. Baffle damping with high amplitude sloshing may present simulation difficulties.

1.0/INTRODUCTION

The S-IVB stage was launched into a nominal 100 mile circular earth orbit on 5 July 1966. This flight (AS-203) provided the most complete data on thermodynamic and fluid dynamic performance of any orbital experiment performed to date. With the data from that experiment, the analytical models available are being verified to determine applicability and degree of correlation. Data from drop tower tests are also being evaluated and compared with analytical models.

Previous presentations of the AS-203 experimental data have been made (Ref. 4 and 5). Particular areas of interest have been determined to be repressurization, pressure rise during coast, liquid level rise bubble dynamics and liquid carryover, and sloshing and settling. During this study, data presented in those reports will be evaluated in conjunction with the analytical models available. Where possible, test data will be compared with analytical predictions. Where models show good correlation with test data, parametric studies will be performed to define the range of operating conditions.

In order to design future upper stage vehicles and extend the operating conditions, i.e. coast times, of present vehicles, it is necessary to confirm the analytical models available. It is the further aim of this study to define areas in which more data is required, either through analytical development or additional experiments.

2.0/TECHNICAL DISCUSSION

Analytical investigations have been conducted in four major areas during this quarterly period. The propellant thermodynamic conditions during repressurization are being evaluated using available computer models. The pressure rise rate during the fourth orbit has been predicted. Both of the above studies use the same methods for evaluation of thermal energy input to the tank. The above studies use different First Law models for pressure history prediction, the particular details of the models are indicated in the following discussion. A model for liquid level rise is presented. In the slosh analysis area, the use of available computer models on a drop tower model tank is presented.

2.1 REPRESSURIZATION FOR AS-203

As discussed in Reference 1 two tools are being applied to the repressurization problem. One method uses the S-II Pressurization Program incorporating thermal evaluation results of the Convair Space Vehicle Radiant Energy Program and the Convair Variable Boundary II Heat Conduction Program.

The Convair Space Vehicle Radiant Energy Program was run for the latter portion of the first orbit and for the initial portion of the second orbit while repressurization occurs. Orbital incident heating rates for the forward cone, dry sidewall and wet sidewall were obtained from this program. These heating rates were input into the Convair Variable Boundary II Heat Conduction Program to obtain the heat flux absorbed by the tank fluid. Because of the discrepancy between predicted and actual heat flux indicated in previous AS-203 flight data evaluation reports, several cases were run in order to simulate the experimental results. Figure 2-1 gives

a comparison of heat flux to the sidewall of the tank with a dry polyurethane foam insulation and with the same insulation impregnated with liquid hydrogen. Although the heat fluxes to the liquid vary significantly due to the different insulation concepts evaluated, the flux to the ullage thru the sidewall and thru the forward dome (not shown) do not vary much within the range of insulation thermal conductivity and specific heat considered. This effect of thermal conductivity is being further investigated (Sec. 2.2). Since the pressure rise rate is much more dependent upon ullage heating rate it is considered that runs should be made using the dry foam properties initially and then if good correlation is not obtained, investigate the case of GH_2 or GH_e impregnated insulation to determine the effect of these property changes. Based on these results the S-II Pressurization Program was input and effort is currently being made to run this for a case with no recirculation. Recirculation will then be added to determine the effect of this flow on the pressure history during repressurization.

The other model being used is an analytical computer model, Convair P3995, which has been modified to include the effects of fuel recirculation. Also modifications were made to handle transient heat transfer through thick walls of two different types of materials and to allow the input of helium flow rate and temperature as a function of time. The tank geometry of the S-IVB was input into the block data section of the program and the program was compiled on the CDC 6400. The S-IVB repressurization case is currently being run.

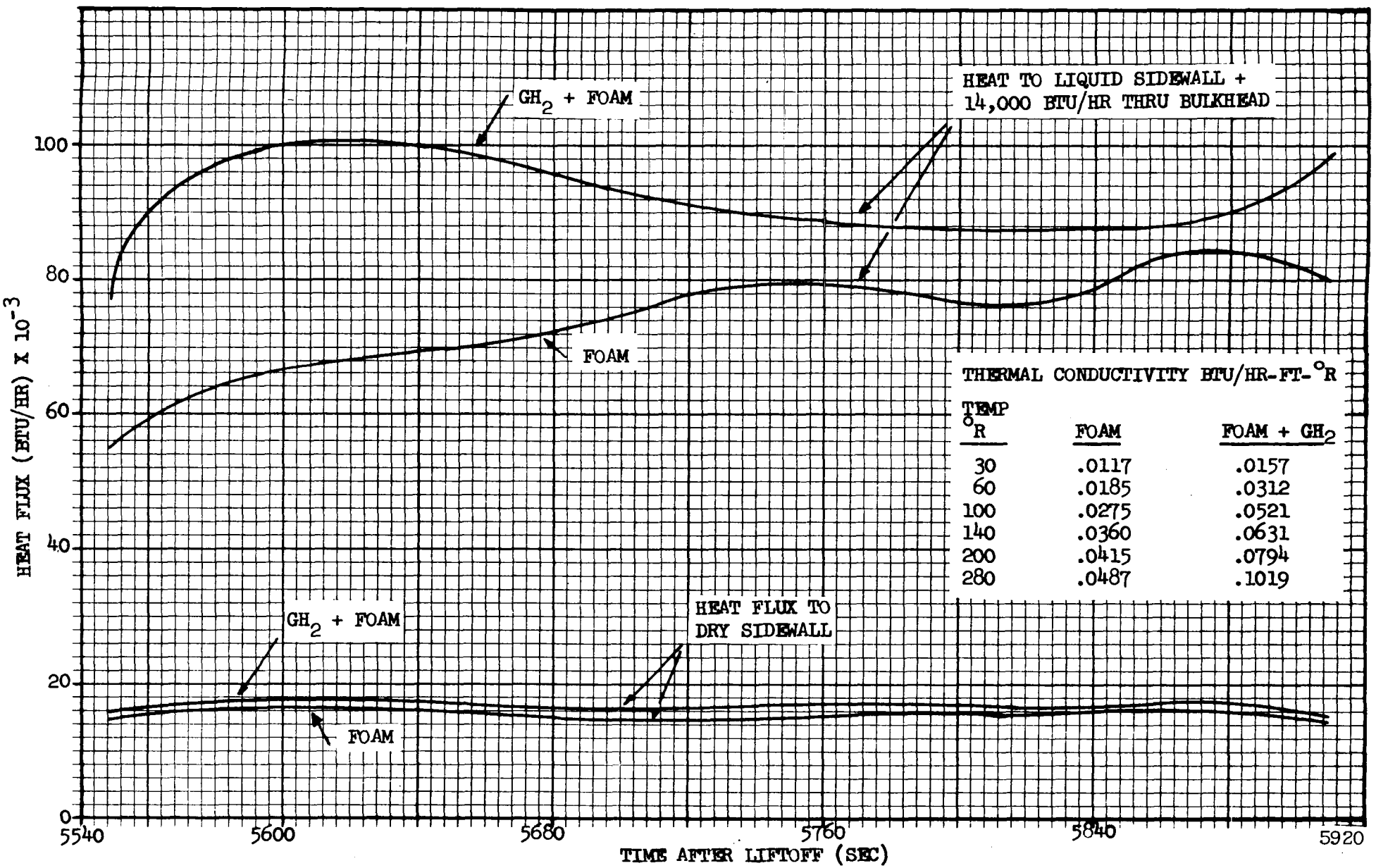

Figure 2-1. Comparisons of Heating Rates for Two Foam Conductivities

2.2 CLOSED TANK PRESSURE RISE

The thermodynamic performance of the hydrogen tank of the AS-203 vehicle was analyzed for the fourth orbit, 17140 seconds to 22,800 seconds range time. After the blowdown to saturated conditions of 12.5 psia prior to 17,140 seconds, the tank was locked up for the above period. Major interest lies in the capability to predict the pressure rise rate over this time period and to further define the contributions of heat flux causing this pressure rise rate. The method of evaluating these heating rates was described in the first quarterly progress report (Ref. 1). The magnitude of incident heat fluxes determined from the Space Vehicle Radiant Energy Program was presented in that report.

During this reporting period, significant emphasis has been placed on the calculation of the energy absorbed by the ullage and by the liquid. In particular, energy transmitted through the forward dome area has proven to be difficult to analyze. This significant parameter will require further evaluation before conclusive results can be obtained on the pressure rise rate. The Convair Variable Boundary II Heat Conduction Program (Ref. 2) is being used in the ullage absorbed energy analysis, while some pressure rise evaluations have been made with the Residual Propellant Orbital Thermodynamic (REPORTER) Program (Ref. 3) developed uner NAS8-20165.

2.2.1 THERMAL ANALYSIS. As indicated in the first quarterly report, for purposes of heat transfer analysis, the S-IVB fuel tank was divided into quadrants and into three axial sections, at STA 555 where the forward bulkhead ends and at STA 445 near the nominal wetted liquid level during fourth orbit, a total of twelve sections. Little difficulty occurred in

the analysis of the lower two sections; however the forward dome area has presented some unusual analytical problems.

The energy input to this forward bulkhead area is by radiation from the forward shroud cylindrical and conical sections. Douglas indicates the forward bulkhead was covered with three layers of aluminized mylar with an aluminized side out having an absorptivity of 0.05. If the mylar side were out, the appropriate absorptivity may have been as high as 0.55. Environmental conditions during the period prior to lift-off may also have resulted in deterioration of the first value to a significantly higher value. Through temperature differences in the forward wall and the magnitude of predicted fluxes, it will be shown to be highly probable that the absorptivity was considerably above 0.05 although possibly not as high as 0.55. Although two or three layers of aluminized mylar may have been used, the outer surface absorptivity is controlling and the inner layers only tend to modify the effective k of the insulation, which is not considered to be a significant variable in ullage heating.

An excellent method to be used in checking the adequacy of propellant tank thermodynamic modeling techniques is to compare the temperature difference measured across the tank wall with that predicted from the computer simulation.

Data obtained for the fuel tank forward bulkhead are used for this modeling correlation. The difference in temperature between the inside and outside surfaces of the bulkhead wall along fin lines I and III at Station 652.7 are shown on Figure 2-2. The temperature differences were obtained from temperature sensors C85 and C328 (fin line I) and C86 and C329 (fin line III) on the AS-203 orbital vehicle.

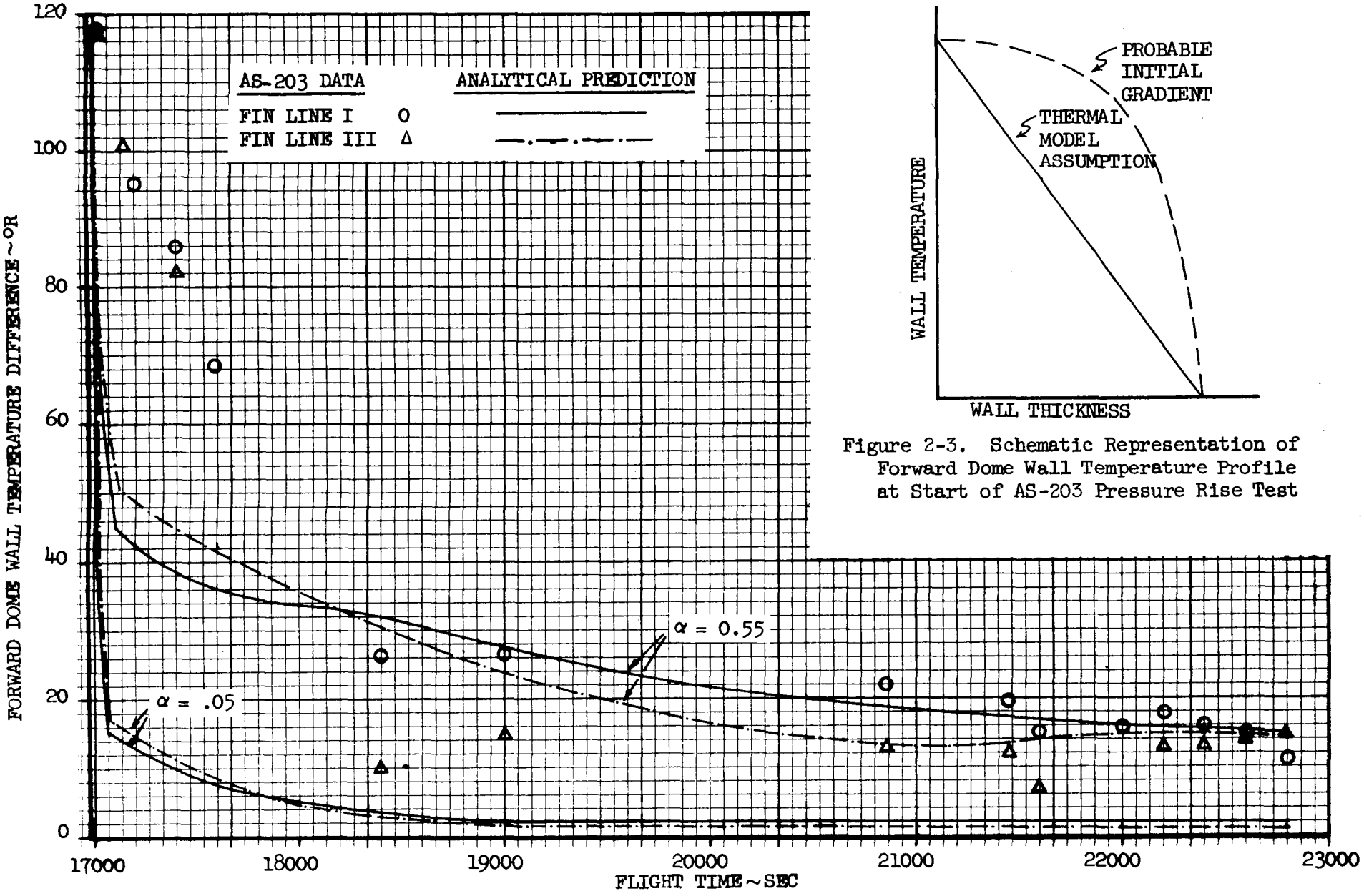

Figure 2-3. Schematic Representation of Forward Dome Wall Temperature Profile at Start of AS-203 Pressure Rise Test

Figure 2.2. Forward Dome Wall Temperature Difference at STA 652.7 for the AS-203 Pressure Rise Experiment

The forward bulkhead was thermally modeled by dividing the dome into quadrants along the fin lines and into four thickness nodes in each quadrant. To determine the thermal energy transferred to the dome from its external environment, radiation view factors were calculated between the dome quadrants and the quadrant sections of both the cylindrical instrumentation unit and forward interstage adapter and the conical nose fairing. A time dependent energy balance was taken on the cylindrical and conical sections and the energy input to the bulkhead calculated by performing a simultaneous energy balance on the dome itself. The bounding heat flux on the outside of the bulkhead was radiative while free convection was assumed to govern the transfer of energy away from the inner dome surface to the gaseous propellant sink for the closed tank calculation. For the free convection calculations, the vehicle acceleration level was varied from 1.05×10^{-2} ft/sec^2 at tank lock-up to 2.35×10^{-3} ft/sec^2 at the time of final loss of communication. These inputs were obtained from AS-203 flight acceleration data.

The proper modeling of the bulkhead thermal energy balance is dependent to a very large part on the use of the correct value of outside surface thermal absorptivity. Since the dome was covered with aluminized mylar, two extreme values for the surface absorptivity are possible. With proper installation of the mylar sheet, aluminized side out, and no degradation of the reflectivity of the vapor deposited aluminum the absorptivity is approximately 0.05. With the sheet installed with the aluminized side in, the absorptivity of the mylar surface is approximately 0.55. Another possibility exists; that is the sheet is installed properly, but the reflectivity of the aluminum surface has been degraded by weathering. In

this case, it is not entirely possible to predict the surface absorptivity. For this investigation, the tank energy balance was made twice using both of the extremum values for dome absorptivity. The acceptability of either value in the thermal modeling was based upon both the comparison of analytical test dome wall temperature differences and tank pressure rise rates. The value of both predicted and experimental temperature differences is shown on Figure 2-2. It is readily apparent that the values obtained with the value of 0.05 are entirely too low and that this value of surface absorptivity is incorrect. On the other hand, the predicted temperature difference values obtained with an absorptivity value of 0.55 are somewhat too high. It appears that the value is somewhere between the two extremes. An investigation is now under way to determine the effective degradation of vapor deposited aluminum absorptivity with weathering. This investigation should provide an answer to the question of proper dome surface conditions to use in the thermal modeling of the tank.

One other modeling problem is apparent from a review of the experimental data in Figure 2-2. The temperature difference decay just prior to and immediately after the start of the closed tank pressure rise test (17140 seconds) is not properly predicted by either set of analytical data. The assumption was made in the thermal model for problem initial conditions that the temperature gradient across the tank dome wall was a straight line as shown in Figure 2-3. Due to the very rapid chilldown of the tank due to a tank venting blowdown and the low conductivity of the tank wall, this assumption may have been incorrect. It appears that the initial wall gradient may have been more nearly shaped like the approximation of Figure 2-3. A gradient of this type would explain the reason for the difference

in slope of the temperature difference decay line between analysis and test. This situation is also under investigation and will be reported later.

The results of the analysis for heating rates through the forward bulkhead are shown in Figure 2-4. The predicted heat flux for the cylindrical side wall sections is shown as a basis of comparison for the predicted magnitude of the forward dome heating. If the absorptivity of .05 had existed, the dome heating would have been almost insignificant. As indicated in Figure 2-4, for absorptivities investigated, the dome heat flux is always less than the cylindrical section, although the dome area exceeds the dry side wall in this case by 18 per cent. Test data points from Reference 4 on Figure 2-4 correlate reasonably well with the cylindrical section prediction. Test data in the dome area suggests the absorptivity value is higher than .05, but as indicated earlier a value of α equal .20 may fit the test data. As the absorptivity on the forward dome increases, the forward bulkhead heating rates become a more significant contribution to ullage heating. From the pressure rise analysis to be discussed later, it appears ullage heating for the closed tank experiment should total about 49,000 BTU. The absorptivities of 0.05 and 0.55 gave respectively 41,000 and 61,000 BTU for ullage heating. The negative heating flux in Figure 2-4 and the inability to match the temperature differences in this area with α = .05 suggest a value of absorptivity near 0.20 may be more appropriate.

The heating rates to the liquid and gas are calculated in the thermodynamic program REPORTER. The heating rates are input to the program as a function of axial location and the program calculates liquid and ullage heating. These heating rates are presented in Figure 2-5 for the ullage

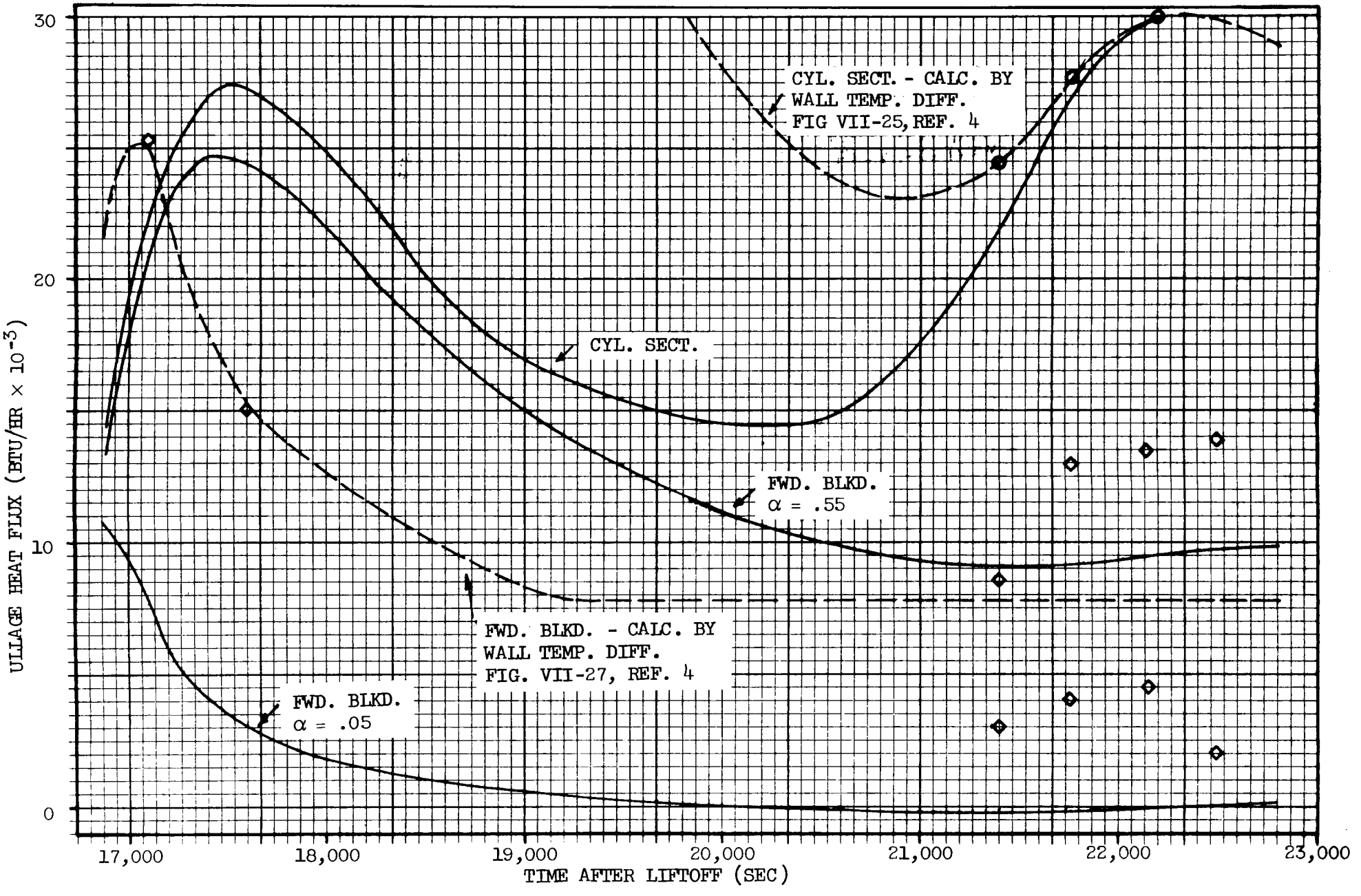

Figure 2-4. Comparison of Ullage Heating Fluxes For Two Absorptivities With AS-203 Data

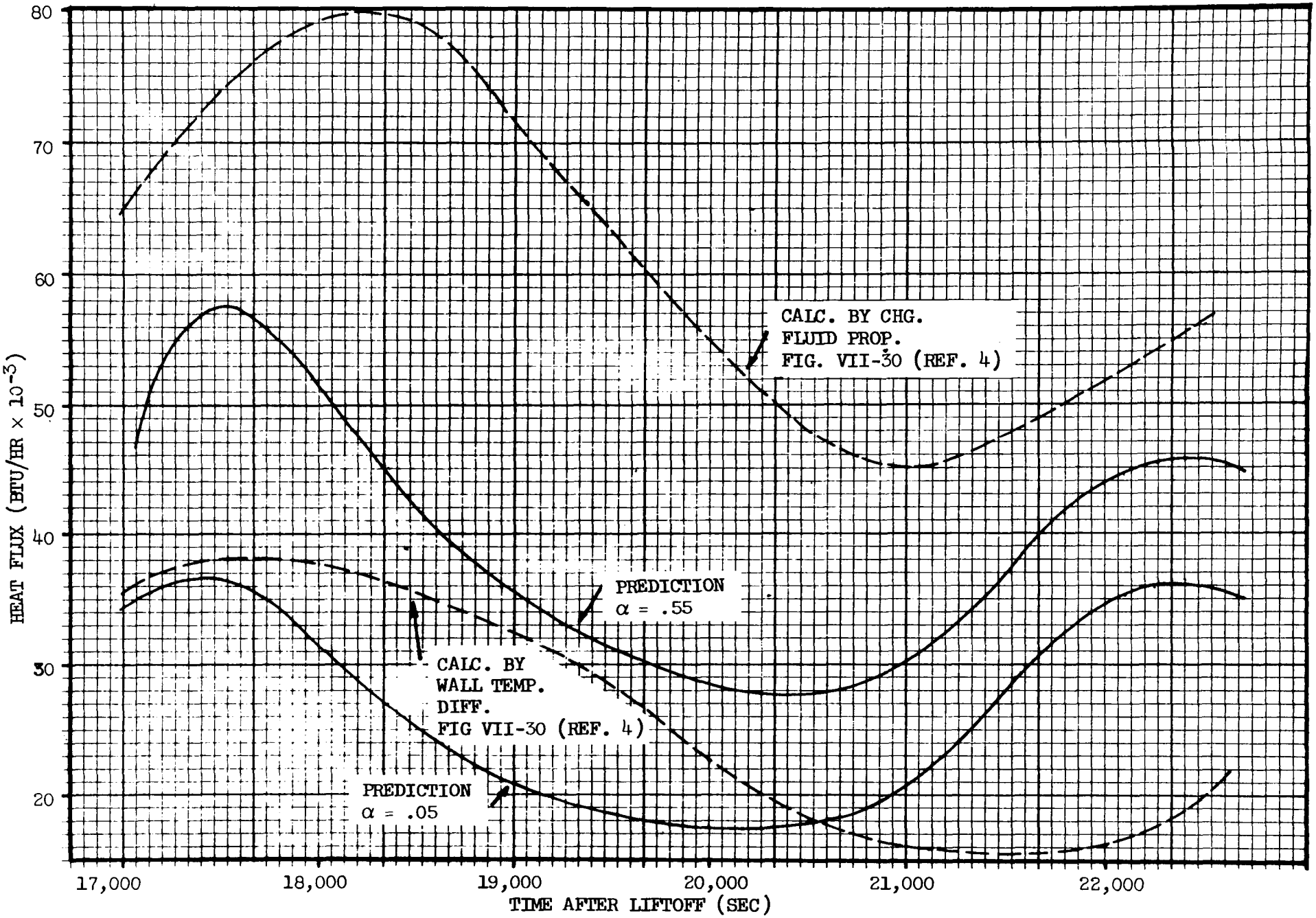

Figure 2-5. Comparisons of Ullage Heat Fluxes With Measured AS-203 Data

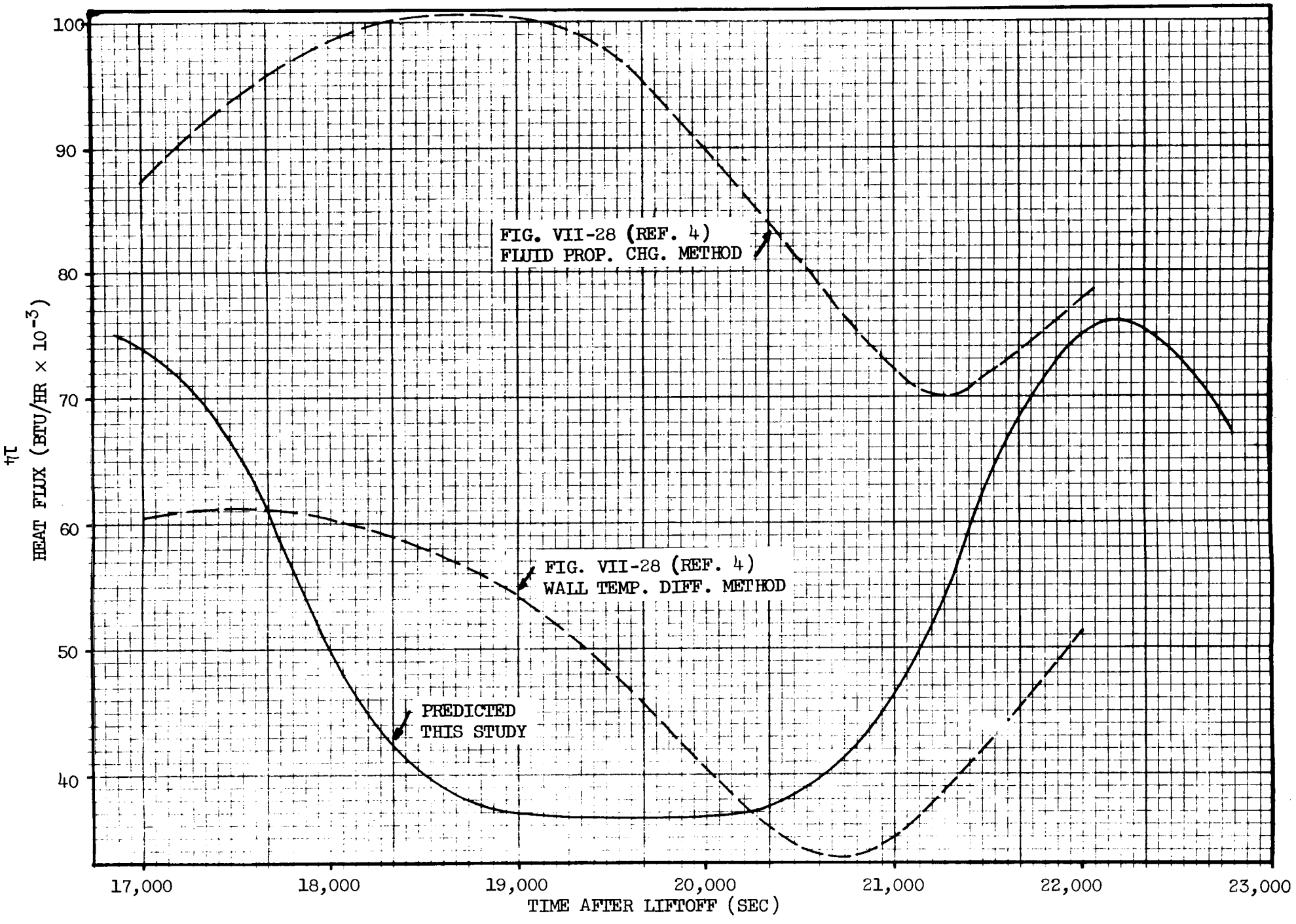

Figure 2-6. Comparison of Liquid Heat Fluxes With Measured AS-203 Data

where a comparison can be made with the results reported in Reference 4. There, two approaches were used in an evaluation of the heating rates, one an evaluation of heating rates through changes in ullage fluid properties, and the other a calculation using measured wall temperature differences and an assumed thermal conductivity. The authors of Reference 4 prefer their results on change of fluid properties since it is in agreement with continuous vent flow , also the thermal conductivity is most likely higher than used in the temperature difference method. The comparison of these two methods with Convair predicted results suggests better agreement for the ullage during the fourth orbit with the wall temperature difference method. Alternatively, the disagreement with the fluid properties evaluation must be resolved. This latter task will be undertaken next quarter.

For liquid heating, predicted results are compared with test data in Figure 2-6. Predicted results compare more favorably with the heat fluxes determined from the wall temperature difference method. Investigators in Reference 5 report a heat input of 79,000 BTU/hr to the liquid using wall temperature difference and 69,000 BTU/hr plus 47,000 BTU/hr boil-off using fluid properties. The predicted value is only 52,000 BTU/hr input to the tank, a value somewhat lower than the other investigators. The differences between predicted values and fluxes from the AS-203 data are still being reviewed.

2.2.2 PRESSURE RISE RATE. The significance of a valid model for thermal analysis is manifested in the ability to predict the pressure rise rate. Other than defining hot spots and maximum temperatures, the thermal analysis is only required to adequately model the thermodynamic state of the fluid. Although it is recognized that the forward bulkhead heating

input requires additional study, some results are presently available on the pressure rise rate prediction.

Although program REPORTER has the capacity for analysis of a 10 node problem permitting stratification in the ullage because of different axial heating rates, the use of a single node problem with one liquid and one ullage node has been found to give similar results to the multi-node configuration for pressure rise rate. In the interest of economy, the single node analysis has been used.

For the two heat flux calculations discussed earlier, i.e. dome absorptivities of 0.05 and 0.55, the heat flux tables are exactly the same for all stations below the dome. It is not unexpected therefore that for the two cases, the liquid thermodynamic states determined with REPORTER are equal. The liquid in both instances remained subcooled during the entire simulation with no evaporation occurring. This is not entirely in agreement with previous investigators.

The differences in ullage heating resulted in different pressure rise rates. These rates are compared in Figure 2-7 with the pressure history of the AS-203 flight for the period of the closed tank experiment. These cases indeed bracket the test data. It remains to determine whether boil-off did occur; if so, the low absorptivity prediction would be increased toward the flight data. It is noteworthy that the degree of subcooled liquid, 5.7^{o}R below the saturated conditions for final test data pressure, indicates increasing liquid heat flux two-fold would not result in a prediction of boil-off with program REPORTER. Thus, to expect a contribution from evaporation with this model is unacceptable and the contribution of boil-off must be added outside the program. This difficulty

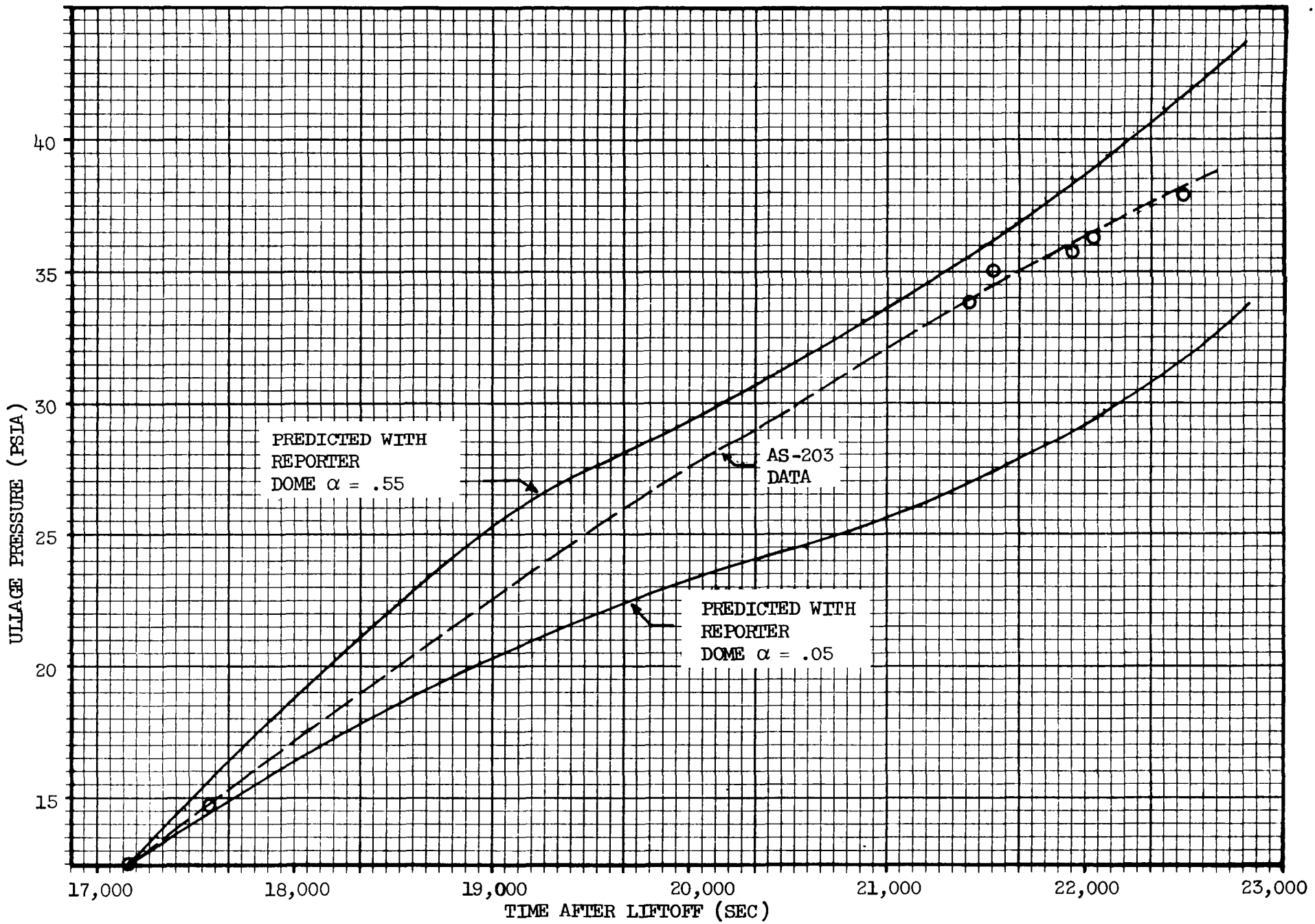

Figure 2-7. Comparison of Predicted Pressures With AS-203 Pressure History

with boil-off contribution has been experienced elsewhere in models which fail to adequately model stratification. The ullage modeling and the boil-off contribution are to be a subject of further investigation when more valid heat flux data has been obtained. Implied differences between the fluid properties or sensible heating evaluation of the ullage and the ullage energy balance in REPORTER will be reviewed.

2.3 DEPRESSURIZATION AND BOILING ANALYSIS

Liquid level rise caused by boiling constitutes a potential problem area for space vehicles utilizing cryogens. The level of a liquid cryogen boiling in a tank increases due to the presence of vapor bubbles entrained in the liquid. The amount of vapor entrainment is enhanced in a low-gravity environment due to a reduction in bubble rise velocity because of a decreased buoyancy force which results in longer bubble residence times in the liquid. The rise problem is particularly serious during pressure relief venting of a tank containing saturated liquid where large quantities of vapor can be generated by boiling caused by a pressure reduction.

A prediction of liquid level rise due to boiling would be desirable in order to prevent liquid boilover during a venting operation. Also, it would be desirable to predict the maximum venting rate that can be tolerated during a rapid blowdown of a cryogenic tank. To date, there is no quantitative data of level rise during venting in a low-gravity environment. A successful design of a cryogenic tank incorporating pressure relief venting depends on the availability of such information. However, before experiments are conducted, it is desirable to have analytical tools available to predict liquid level rise during a venting

operation. The development of these tools is the purpose of this study.

A purely analytical approach to the problem of liquid level rise will be employed here. The study will employ the basic equations of motion and heat transfer. At the present time, there are few analytical investigations of liquid level rise (Ref. 6, 7, 8). This is probably because certain unknowns are rather difficult to describe analytically. These involve determining the amount of energy that goes into vapor production and quantity of vapor that remains entrained in the liquid during a venting operation. The first unknown involves describing bubble nucleation, growth, and departure at a solid surface and liquid-vapor interface, while the second entails describing the motion, interaction, and coalescence of individual bubbles in a liquid. Also, there are problems related to determining the relative importance of nucleation at a solid surface, liquid-vapor interface, and impurities in the liquid bulk. The above problems which previous investigations have neglected or simplified are being examined in this study.

This phase of the study is concerned with indicating the possible magnitude of liquid rise under certain simplifying assumptions. Equations are derived to determine the quantity of liquid mass evaporated allowing for saturation pressure change, liquid superheat, and wall heat transfer. From the evaporated mass, equations are developed to predict liquid level rise in terms of an unknown parameter. This parameter describes the amount of vapor that remains entrained in the liquid and is related to the nucleation process, motion and interaction of bubbles. Depending on the magnitude of entrained vapor, significant liquid level rise is predicted. Future analyses will be directed towards predicting the quantity

of entrained vapor which will comprise examination of bubble nucleation and subsequent motion in the liquid.

2.3.1 ANALYTICAL MODEL. Consider a cylindrical tank of height H that is initially filled with liquid to a height h_o. The entire liquid remains saturated and settled in the bottom of tank during the course of a venting operation in which the saturation pressure decreases. The reduction in mass of saturated liquid by evaporation and subsequent liquid rise due to vapor entrainment are to be determined for different levels of pressure reduction. Also, estimates of the effects of liquid superheat and wall heat transfer are to be determined.

2.3.1.1 Level Rise Due To Pressure Reduction. The quantity of liquid mass evaporated by boiling due to a saturation pressure reduction can be determined from an energy balance on a saturated liquid given as:

$$-\lambda dm = mC_s\, dT \tag{1}$$

where heat transfer, liquid superheat, and variable properties have been neglected. Integrating Equation 1 between initial and final states yields:

$$\frac{m_f}{m_o} = \exp\left(-\frac{C_s}{\lambda}\Delta T_s\right) \tag{2}$$

If a fraction β of vapor generated over the reduction in pressure remains entrained in a settled liquid, the increase in liquid height due to bubble displacement is given as:

$$\Delta h = \frac{\beta(m_o - m_f)}{\rho_v A_c} \qquad (4)$$

where β has been assumed to remain constant over the duration of a venting operation. This is not exactly true due to the unsteady nature of the nucleation process, location of nucleation, and bubble motion in the liquid. Future analyses will examine these interactions. For now, however, β will be assumed to represent some average quantity of vapor entrained in the liquid during the time interval of a vent cycle. From the summation of Equations 3 and 4, the liquid height corresponding to a change in saturation pressure and vapor entrainment is given by:

$$\frac{h}{h_o} = \exp\left[-\frac{C_s}{\lambda}\left(\frac{\overline{dT}}{dP}\right)\Delta P\right] + \beta\frac{\rho_\ell}{\rho_v}\left\{1 - \exp\left[-\frac{C_s}{\lambda}\left(\frac{\overline{dT}}{dP}\right)\Delta P\right]\right\} \qquad (5)$$

where an average slope of the saturated liquid-vapor pressure curve has been employed.

Calculations which have been performed utilizing Equation 5 are presented in Figure 2-8. Average liquid hydrogen properties were used over a pressure range of 10-50 psia and are given as:

$$C_s = 2.5\ \frac{BTU}{lb_m\ ^oR} \qquad \rho_\ell = 4.30\ \frac{lb_m}{cu\ ft}$$

$$\lambda = 188\ \frac{BTU}{lb_m} \qquad \rho_v = 0.123\ \frac{lb_m}{cu\ ft}$$

$$\left(\frac{\overline{dT}}{dP}\right) = 0.300\ \frac{^oR}{psi}$$

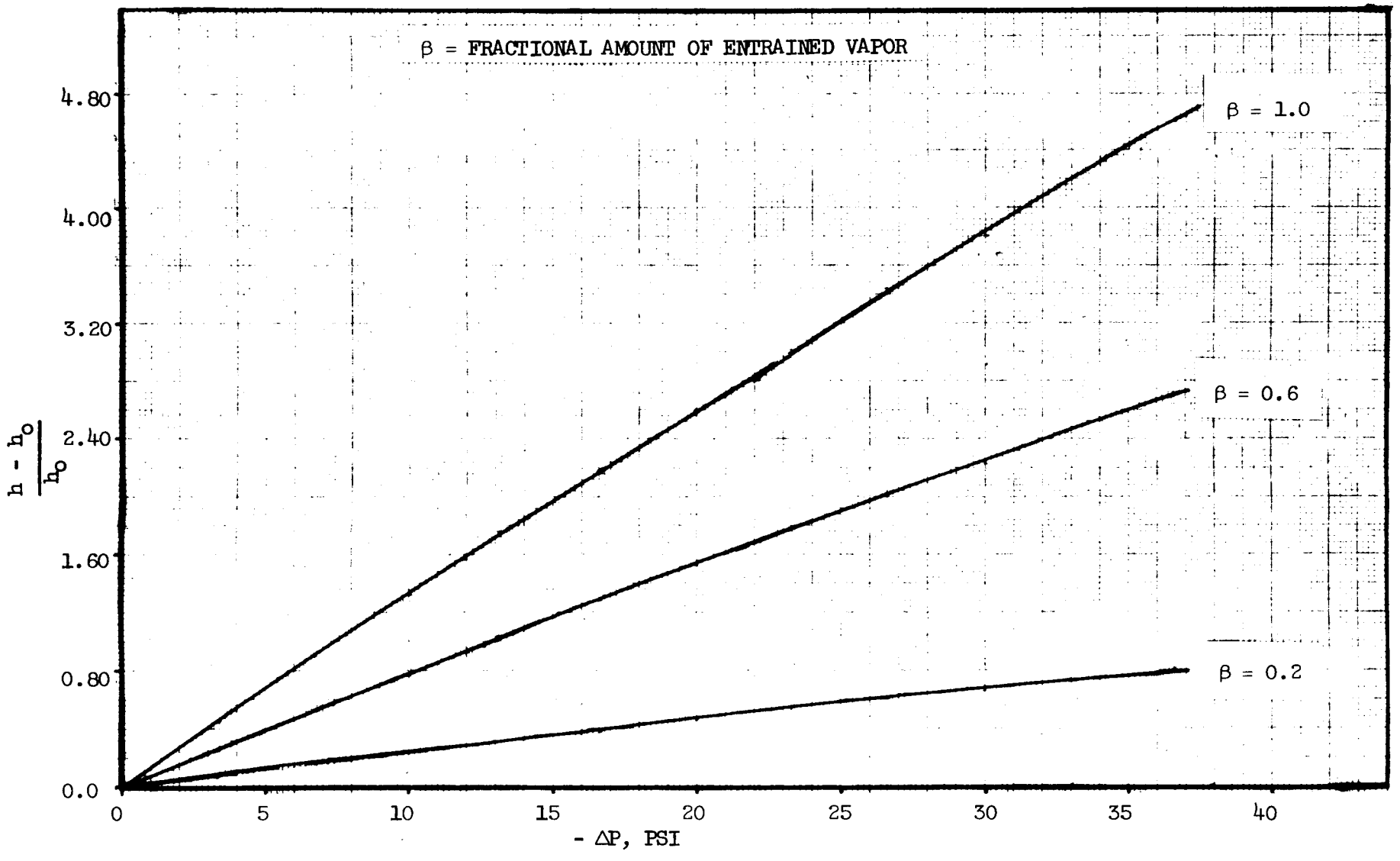

Figure 2-8. Relative Liquid Level Rise Vs. Pressure Reduction

It is noted in Figure 2-8 that potentially serious liquid level rise problems can occur for high pressure reductions, depending on the quantity of entrained vapor. For example, for a pressure reduction of 26 psi where 60 per cent of the vapor generated remains entrained, the liquid level rise would be twice the initial fill level.

To determine the maximum allowable pressure reduction for venting a tank of height H initially filled to a level h_o, without liquid reaching the top of the tank, Equation 5 is solved for ΔP_{max} corresponding to $h = H$ to yield

$$\Delta P_{max} = - \frac{\lambda}{C_s} \left(\frac{\overline{dP}}{dT}\right) \ell n \left[1 - \left(\frac{H}{h_o} - 1\right)\left(\frac{1}{\beta \frac{\rho_\ell}{\rho_v} - 1}\right)\right] \qquad (6)$$

Calculated results using Equation 6 with the previously given LH_2 properties are presented in Figure 2-9. This figure shows that the magnitude of pressure relief during a one cycle blowdown can be very small depending on the fill level and quantity of entrained vapor. It is not unlikely that multiple vent cycles would have to be employed to reach a required pressure reduction if β were near one.

It should be noted here that two conservative assumptions are made in the design of vehicles utilizing pressure relief venting of a cryogenic container. These are:

1. That all the heat input into the tank is absorbed in vapor generation
2. That all the vapor generated remains entrained in the liquid.

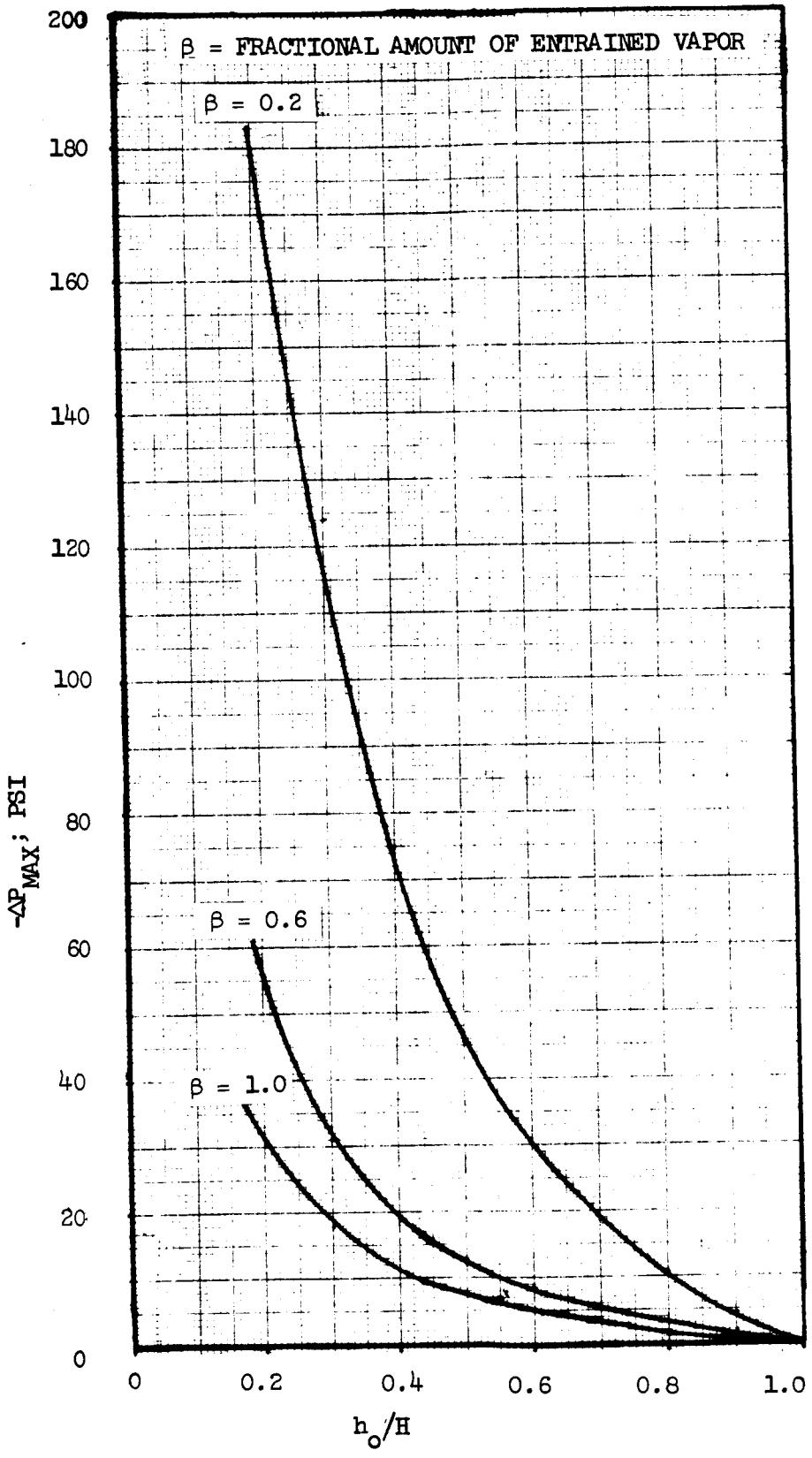

Figure 2-9. Maximum Pressure Drop Relationship For Fractional Fill Levels

From the analysis of the S-IVB vent-downs during the AS-203 flight (Ref. 1), it is believed that both of these assumptions are overly conservative and place severe restrictions on venting a propellant tank as can be seen from the $\beta = 1$ curves of Figures 2-8 and 2-9. Future analyses will examine both of these assumptions to predict their quantitative importance.

2.3.1.2 Effects of Liquid Superheat. Before boiling occurs, the liquid temperature must increase above the saturation temperature due to surface tension effects. The degree of superheat required is dependent on liquid properties, operating pressure, and geometry of the nucleation site. To account for the energy which can be absorbed in liquid superheat, Equation 1 is modified as:

$$m'C_s \Delta T_i - \lambda dm = mC_s dT \tag{7}$$

Dividing through by m and integrating Equation 7 between initial and final states corresponding to a saturation temperature change yields for the final liquid mass

$$\frac{m_F}{m_o} = \exp\left[- \frac{C_s}{\lambda} \left(\Delta T_s - \psi \Delta T_i \right) \right] \tag{8}$$

where $\psi \equiv m'/m$ is assumed constant. Equation 8 relates how liquid superheat reduces the amount of evaporation since part of the energy released due to a saturation pressure reduction is absorbed in superheating the liquid. Similar to the derivation of Equation 5, the liquid level rise due to pressure reduction with superheat effects included is given as:

$$\frac{h}{h_o} = \exp\left[- \frac{C_s}{\lambda}(\Delta T_s - \psi \Delta T_i)\right] + \beta \frac{\rho_\ell}{\rho_v}\left\{1 - \exp\left[- \frac{C_s}{\lambda} (\Delta T_s - \psi \Delta T_i)\right]\right\} \tag{9}$$

To determine the magnitude of superheat that a liquid can sustain before boiling, the following expression developed in Reference 9 for a bubble growing in a solid cavity will be used

$$\Delta T_i \simeq \frac{R_v T_s^2}{J \lambda} \frac{2\sigma}{r P_\ell} \tag{10}$$

Using saturated LH_2 properties corresponding to a pressure of one atmosphere and a cavity radius of 10^{-4} in. which is typical for most surfaces, the amount of superheat is determined to be $0.116^{\circ}R$. This result is consistent with the values measured in Reference 10. Using this value of superheat in Equation 9 and assuming all the liquid is superheated ($\lambda = 1$) results in a 12 per cent reduction in level rise for a $1^{\circ}R$ reduction in saturation temperature and $\beta = 0.6$. It should be noted that a $2.5^{\circ}R$ superheat was required to initiate boiling of LH_2 in Reference 11 which employed a different surface material and preparation than that of Reference 10. This indicates that surface effects can be important. If this higher value of superheat is attainable for LH_2 and nucleation at a solid surface is the main contributor to vapor production, then, superheat effects can become very important as a factor in delaying and reducing LH_2 level rise.

2.3.1.3 Influence of Wall Heat Transfer. Heat transfer through the walls of a cryogenic tank containing saturated liquid is another mechanism for vapor generation. To account for wall heat transfer, the energy equation

for a saturated liquid is given as:

$$\delta Q_w + \lambda dm = - mC_s\, dT \tag{11}$$

Dividing through by m, approximating

$$\frac{\delta Q_w}{m} \simeq \frac{\delta Q_w}{m_o} \quad \exp\left(\frac{C_s}{\lambda} \Delta T_s \right) \tag{12}$$

from the use of Equation 1, and integrating Equation 11 between initial and final states for constant heat transfer results in:

$$\frac{m_f}{m_o} = \exp \left\{ - \frac{1}{\lambda} \left[C_s\, \Delta T_s + \frac{\Delta Q_w}{m_o} \exp\left(\frac{C_s\, \Delta T_s}{\lambda} \right) \right] \right\} \tag{13}$$

Equation 13 shows how wall heat transfer results in increased vapor production. As derived previously, the liquid level rise due to pressure reduction with constant wall heat transfer is given as:

$$\frac{h}{h_o} = \exp \left\{ - \frac{1}{\lambda} \left[C_s\, \Delta T_s + \frac{\Delta Q_w}{m_o} \exp\left(\frac{C_s\, \Delta T_s}{\lambda} \right) \right] \right\}$$

$$+ \beta \frac{\rho_\ell}{\rho_v} \left\{ 1 - \exp \left[- \frac{C_s}{\lambda} \Delta T_s - \frac{\Delta Q_w}{\lambda m_o} \exp\left(\frac{C_s\, \Delta T_s}{\lambda} \right) \right] \right\} \tag{14}$$

Using the following values in Equation 14 which are representative of the third orbit, first vent-down of the S-IVB LH_2 tank during the AS-203 flight:

$\dot{Q}_w$ = 25 BTU/sec

ΔT = 180 sec

m_o = 16,300 lb_m

$\Delta Q_w \simeq$ 4500 BTU

results in a 11 per cent increase in level rise due to wall heat transfer for a change in saturation temperature of $1^{\circ}R$ and $\beta = 0.6$. For heating rates near the value used here and larger saturation temperature changes, the influence of wall heat transfer on level rise becomes negligible as compared to pressure reductions by venting.

2.3.1.4 Consideration of Both Superheat and Wall Heat Transfer. From the analysis presented in the previous two sections, the influence on a saturated liquid of both liquid superheat and wall heat transfer can be accounted for by consideration of the following energy balance:

$$-\delta Q_w + m' C_s \Delta T_s - \lambda dm = m C_s dT \qquad (15)$$

Dividing through by m, using the approximation given in Equation 12, and integrating between initial and final states yields:

$$\frac{m_f}{m_o} = \exp\left\{-\frac{1}{\lambda}\left[C_s \Delta T_s - \tfrac{1}{2} C_s \Delta T_i + \frac{\Delta Q_w}{m_o} \exp\left(\frac{C_s \Delta T_s}{\lambda}\right)\right]\right\} \qquad (16)$$

Equation 16 indicates how liquid superheat and wall heat transfer oppose each other in terms of vapor production. The liquid level rise due to saturation temperature change with liquid superheat and wall heat transfer included is determined to be

$$\frac{h}{h_o} = \exp\left\{-\frac{1}{\lambda}\left[C_s\,\Delta T_s - \tfrac{1}{4}C_s\,\Delta T_i + \frac{\Delta Q_w}{m_o}\exp\left(\frac{C_s\,\Delta T_s}{\lambda}\right)\right]\right\}$$

$$+ \beta\frac{\rho_\ell}{\rho_v}\left\{1 - \exp\left[-\frac{C_s\,\Delta T_s}{\lambda} + \frac{\tfrac{1}{4}C_s\,\Delta T_i}{\lambda} - \frac{\Delta Q_w}{\lambda m_o}\exp\left(\frac{C_s\,\Delta T_s}{\lambda}\right)\right]\right\} \quad (17)$$

Substituting the values used for superheat and wall heat transfer used in Sections 2.3.1.2 and 2.3.1.3 results in a 1 per cent reduction in LH_2 level rise for a saturation temperature change of $1^{\circ}R$. This corresponds to the 12 per cent reduction due to superheat and 11 per cent increase caused by wall heat transfer. Therefore, from the results determined here, the effects of superheat and wall heat transfer on LH_2 level rise are negligible compared to saturation pressure reductions.

2.3.2 FUTURE ANALYSIS. In the previous analyses on liquid level rise, the quantity of entrained vapor was left as an unknown parameter and has been assumed to remain constant with time during the period of a venting cycle. To remove these shortcomings, further study of the basic phenomena involved in a venting process will continue. These phenomena include bubble nucleation, growth, rise, interaction, and coalescence. Also, the relative importance of nucleation at a surface, liquid-vapor interface, and in the liquid bulk will be examined.

After the above time-dependent bubble phenomena have been resolved, the unsteady nature of liquid level rise can be examined. From the determination of bubble size and spatial distributions as a function of time during a vent-down, the rate of liquid rise can be determined for various vent flow rates. Maximum vent rate and quantity of vented vapor

can then be determined before boilover occurs for various fill levels and gravity values.

2.4 PROPELLANT SLOSHING ANALYSIS

Propellant sloshing analyses during the second quarter have been concentrated on a theoretical analysis of drop tower scale model slosh testing (Ref. 12). Work is also continuing on the theoretical correlation with AS-203 flight results. In the latter area the six degree of freedom coast phase slosh simulation is being modified to simulate the S-IVB-203 attitude control system. The drop tower slosh data is valuable in that it enables a direct evaluation of the propellant slosh theoretical solution.

A digital computer program has been set up to simulate the drop tower propellant sloshing dynamics. The simulation uses the pendulum analogy to duplicate the sloshing dynamics, provision is included for three slosh modes. The pendulum analogy parameters and the basic mathematical model are shown in Figure 2-10. Figure 2-11 illustrates the slosh parameters as a function of the propellant level showing the sloshing mass and pendulum length. The analytical procedure will be the same as that employed in the actual test. Sloshing will be induced in a one "g" environment, then the acceleration will be reduced to a low level. Data will be obtained on propellant slosh wave amplitude, velocity and acceleration. This data will enable determination of the amplification factor, effective propellant damping, and slosh period as a function of Bond number and Froude number.

Baffle damping is simulated in the form of energy dissipation as an instantaneous function of time. This technique has proved adequate for

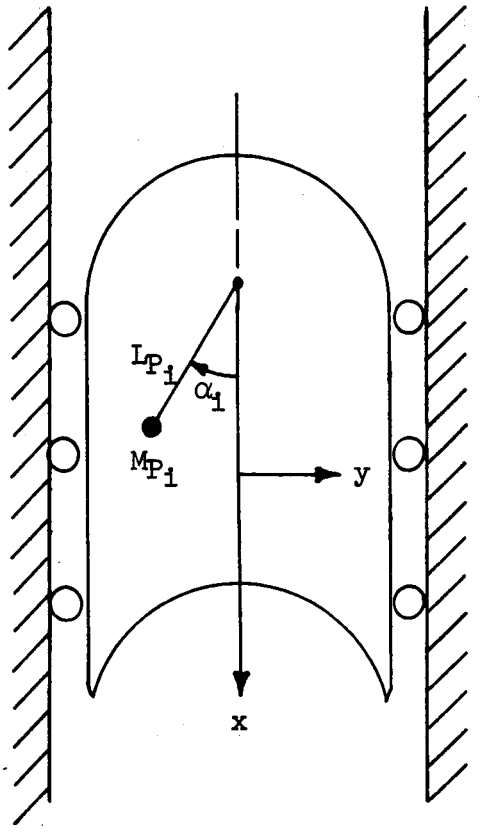

L_{P_i} Pendulum length used in the pendulum analogy for the i^{th} mode sloshing.

M_{P_i} Sloshing propellant mass used as the propellant mass in the pendulum analogy for i^{th} mode sloshing.

α_i Pendulum displacement angle for i^{th} mode sloshing.

Figure 2-10. Drop Tower Propellant Slosh Analogy Parameters.

analysis of Centaur low "g" slosh conditions. Difficulty is anticipated however for the no baffle case, since conventional theory predicts only wall wiping damping, in the absence of an anti-slosh device. This damping, is adequate for low amplitude slosh but inadequate for large amplitudes. Large amplitude slosh gains additional energy losses from turbulence, mixing, etc. If an analytical damping expression for the clean tank configuration is not sufficient to correlate with observed test results then the nonlinear damping coefficient will be parameterized to fit the observed test data.

In summary it is believed that the drop tower test data available presents the best opportunity for correlation of the theoretical analysis

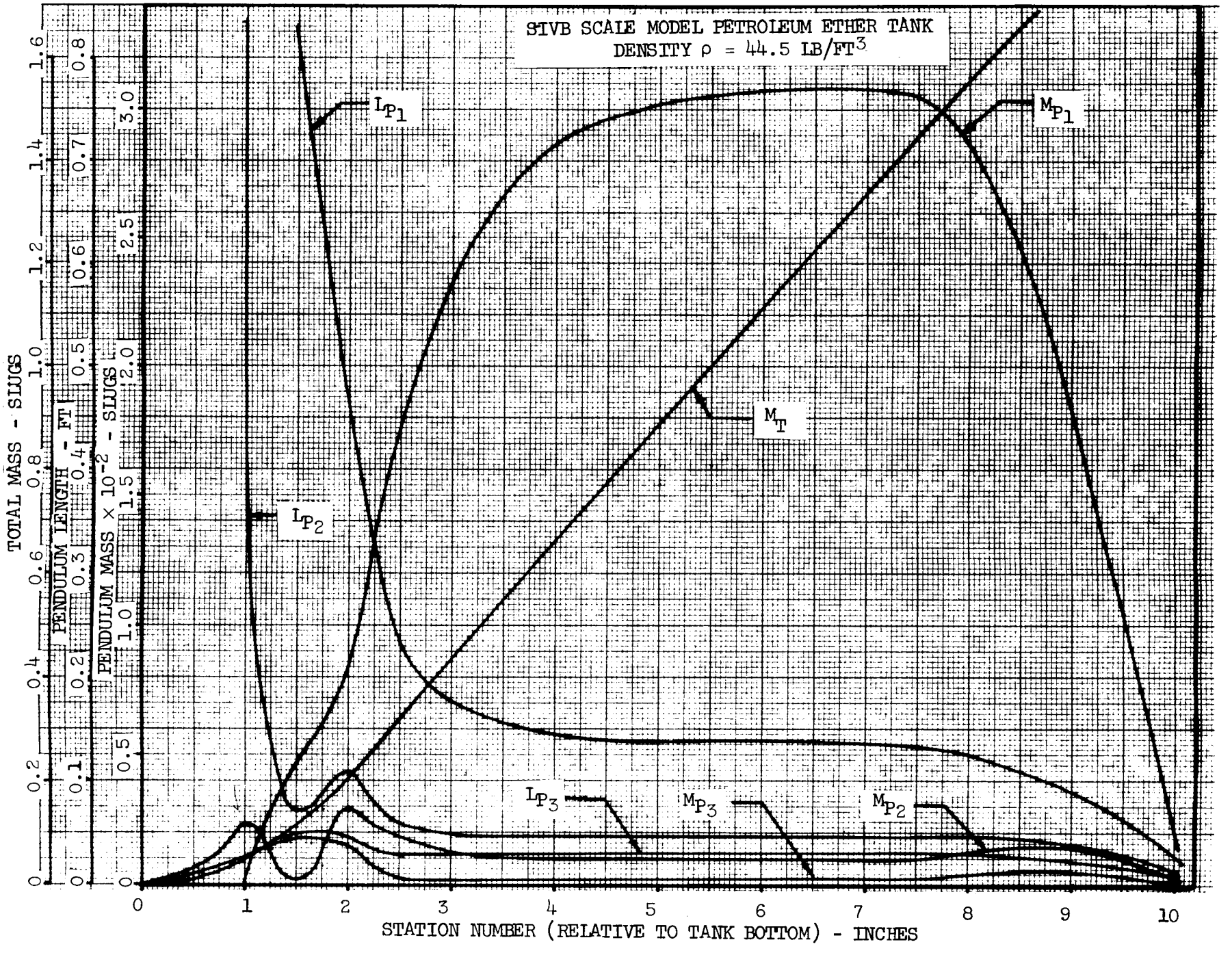

Figure 2-11. S-IVB Scale Model LH_2 Tank Slosh Parameters As a Function of Propellant Level

with test results. This comparison will serve to point out the slosh model inaccuracies and point out problem areas before simulating the AS-203 flight.

3.0/CONTRACT STATUS

3.1 ANTICIPATED PROBLEM AREAS

At the present time, there are no technical problems which are impeding the progress of the study. The study schedule is shown in Figure 3-1 with the points of progress indicated for the six task descriptions. Work reported herein covers work completed during the second quarterly work period. Initiation of the propellant transfer analysis will be delayed until November.

3.2 FUTURE WORK PLAN

During the next monthly reporting period, the comparisons will be made between the two analytical models available for repressurization analysis. Thermal properties for the evaluation of energy input through the forward bulkhead of the AS-203 flight will be defined and the final comparisons for predicted heat fluxes with test data will be completed. The evaluation of pressure rise rate will be continued. The analytical model for liquid level rise during depressurization will be programmed and a parametric study of variables will be made. The importance of bubble phenomena will be defined and the results will be used to improve the analytical model. The dynamics of sloshing study will continue for the drop tower data which models the AS-203 flight.

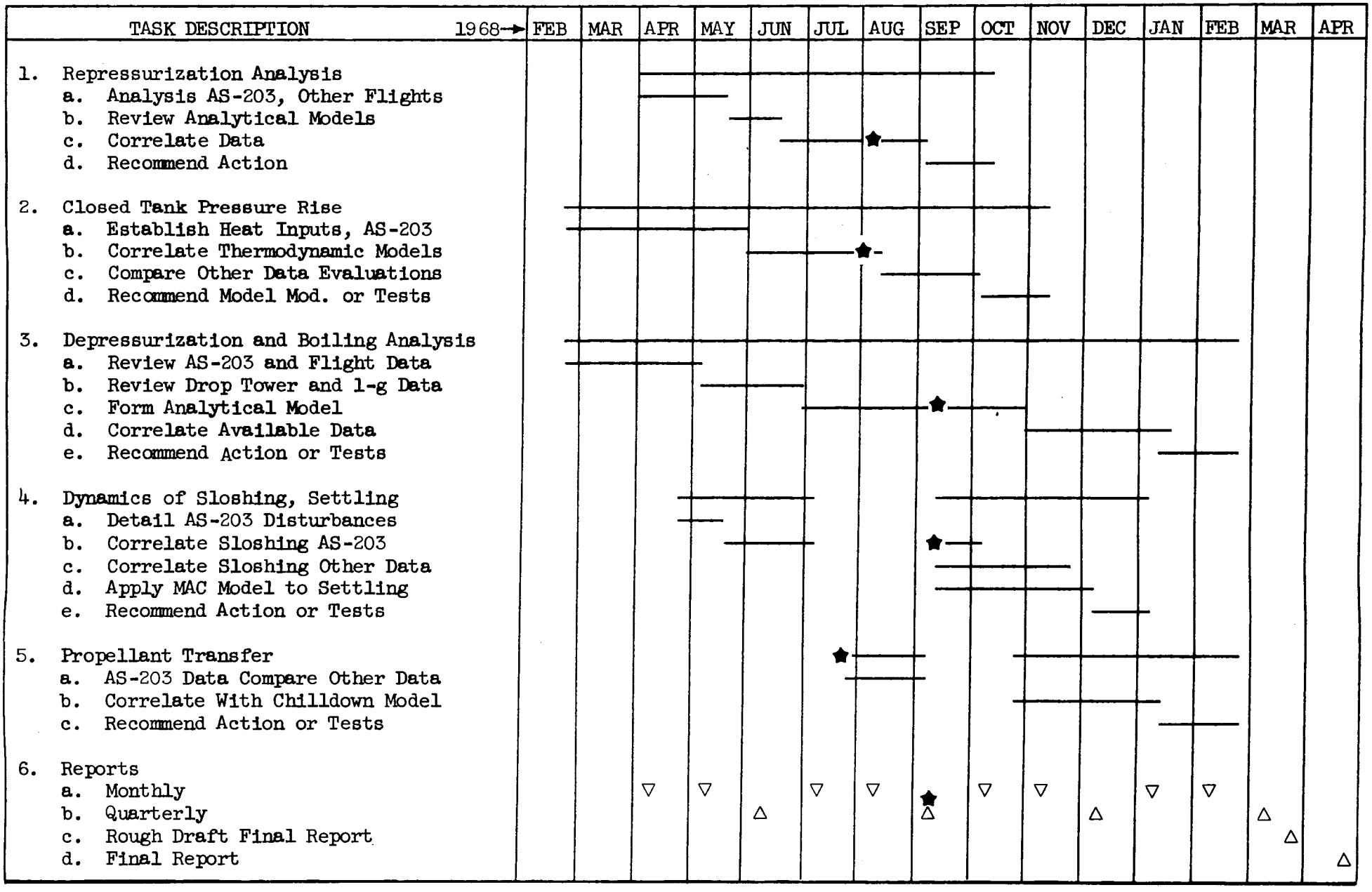

Figure 3-1. Task Schedule for Evaluation and Application of Data From Low-Gravity Orbital Experiment (NAS8-21291)

4.0/REFERENCES

1. Anon.: Evaluation and Application of Data From Low-Gravity Orbital Experiment - First Quarterly Progress Report. GDC Report 584-4-184, Contract NAS8-21291, June 1968.

2. O'Neill, R. F., Worscheck, G. A., and Kramer, J. L., Variable Boundary II Heat Conduction Program. Convair Report GDC-BTD67-004, Contract NAS3-8711, August 1967.

3. Walburn, A. B., and Evans, E. A., Residual Propellant Orbital Thermodynamics Program (REPORTER) Version A. Convair Report GDC-DDB67-004, Contract NAS8-20165, November, 1967.

4. Anon.: Evaluation of AS-203 Low Gravity Orbital Experiment. Chrysler Corp. Report BB-3.4.3-S-101, Contract NAS8-4016, January 1967.

5. Anon.: Saturn S-IVB-203 Stage Flight Evaluation Report, Volume II. Douglas Report SM-46988, October 1966.

6. Adelberg, M., Level of a Boiling Liquid in a Low-Gravity Environment. J. of Spacecraft and Rockets, 5, No. 1, 108, 1968.

7. McGrew, J. L., and Larkin, B. K., Cryogenic Liquid Experiments in Orbit - Vol. II. NASA CR-652, December 1966.

8. Swalley, F. E., Platt, G. K., Hastings, L. J., Saturn V Low Gravity Fluid Mechanic Problems and Their Investigation by Full-Scale Orbital Experiment. Proceedings of Symposium on Fluid Mechanics and Heat Transfer Under Low Gravity, Palo Alto, California, June 1965.

9. Rohsenow, W. M., and Choi, H., Heat, Mass, and Momentum Transfer, P. 217, Prentice-Hall, Inc., (1961).

10. Fredreckson, G. O., Schweikle, J. D., Thermo and Hydrodynamic Experiment Research Module in Orbit, Final Report. DAC-60594, March 1967.

11. Shirley, J. E., Final Report for the General Dynamics/Astronautics Zero-G Program Covering the Period from May 1960 through March 1962. Convair Report FY62-0031, NAS8-2664, August 1962.

12. Toole, L. E., and Hastings, L. J., An Experimental Study of the Behavior of a Sloshing Liquid Subjected to a Sudden Reduction in Acceleration. NASA TM X-53755, August 1968.